Journal of Environmental Chemical Engineering 6 (2018) 549–559

Contents lists available at ScienceDirect

Journal of Environmental Chemical Engineering

journal homepage: www.elsevier.com/locate/jece

CO_2 removal using amine-functionalized kenaf in pressure swing adsorption system

K.S.N. Kamarudin[a,*], N. Zaini[b], N.E.A. Khairuddin[a]

[a] Faculty of Chemical and Energy Engineering, Universiti Teknologi Malaysia, 81310 UTM Skudai, Johor, Malaysia
[b] Malaysian-Japan International Institute of Tecnology, Universiti Teknologi Malaysia, Jalan Sultan Yahya Petra, 54100 Kuala Lumpur, Malaysia

ARTICLE INFO

Keywords:
Kenaf
Amine
Impregnation
Adsorption
Carbon dioxide

ABSTRACT

An agro-based adsorbent from kenaf (*Hibiscus cannabinus* L.) for CO_2 removal was prepared by functionalizing it with amine. Amine functionalization improves the adsorbates–adsorbent interaction through the presence of basic active sites on the adsorbent surfaces. Several amines (MEA, DEA, MDEA, AMP, PEI, DETA, TETA, TEPA, DIPA, PEHA, TEA, and DGA) have been selected for the amine-screening process. The result revealed that adsorption capacity of raw kenaf is only 0.624 mmol/g, whereas TEPA attained the highest CO_2 capture capacity (0.914 mmol/g). Further study on the effect of amine loadings was conducted using two types of amine (MEA and TEPA) and it was found that the highest CO2 adsorption capacity for is 2.070 mmol/g for MEA to kenaf ratio of 1:1 and 2.086 mmol/g for TEPA to kenaf ratio of 2:1. The regeneration study also showed that kenaf sorbent can be used for repeated cycle operations. Due to the presence of amine on kenaf, the regeneration values of MEA–kenaf (82.15%) and TEPA–kenaf (75.62%) were lower than the raw kenaf (99.07%).

1. Introduction

Carbon dioxide (CO_2) capture has attracted global attention due to increasing adverse effects of CO_2 emissions. These emissions are generated from anthropogenic activities during the processing and utilization of fossil fuels (natural gas, coal and crude oil) for transportation and residential purposes. There are many research focused on limiting the greenhouse gas emissions using techniques such as chemical and physical absorption, membrane separations, pressure swing adsorption (PSA), and cryogenic separation processes [1–8]. Consequently, choosing effective method for CO_2 removal is essential to reduce or limit CO_2 emission. Amongst those methods, absorption with amine based solvents is a well developed technology and commonly used in separating CO_2 from flue gas and natural gas stream. However, the high power consumption for regenerating the amine leads to poor overall thermal efficiency [9]. In addition, amine also contributes to corrosion problem that can potentially strike the steel [10,11].

Based on this problem, adsorption on solid materials merit consideration by its simplicity, efficient, and affordable [12,13]. The emergence of various sorbents for CO_2 capture such as commercial activated carbons, molecular sieves, zeolites, and metal–organic frameworks (MOFs) have attracted more investigations into the viability, stability, and design of full scale adsorption process. However, the main challenge remains, finding a solid adsorbents and suitable conditions that promote high capacity and selectivity. Though some of the reviewed commercial adsorbents performed well for the CO_2 adsorption capacity and selectivity, they also demonstrate some weaknesses that remain as a challenging task for commercial application. The existing commercial adsorbents such as activated carbon, zeolites, metal organic frameworks, mesoporous nanoparticles (eg. MCM-41, SBA −15) are costly, require multi–step fabrication procedures, high regeneration temperature, some materials are sensitive to NO_x, SO_x, and H_2O, low adsorption capacity at mild operating conditions (0.1–1 bar and 0–100 °C), low selectivity in gas mixtures, and low the adsorption capacity after multiple cyclic operations [14–22]. These weaknesses would limit the application of these adsorbents in future. For a solid adsorbent, utilization of agro-based material is always attractive because it is less harmful and more benign to the environment than ceramics, metals, metal oxides, and other notorious source of materials. Therefore, attention on the agricultural material for the production of low–cost adsorbent to replace the commercial adsorbent has grown rapidly. Moreover, the encouragement towards low–cost adsorbent began since the economic crisis of the 2000 s that led researchers to turn their interest on the alternative sources over the commercial adsorbents [23]. Table 1 summarized CO_2 adsorption performance of different types of agro-based adsorbents. The adsorbents have been converted into char or activated carbon and treated with different types of chemicals.

* Corresponding author.
E-mail address: r-sozana@utm.my (K.S.N. Kamarudin).

https://doi.org/10.1016/j.jece.2017.12.040
Received 5 September 2017; Received in revised form 28 November 2017; Accepted 18 December 2017
Available online 20 December 2017

Table 1
CO_2 adsorption capacity of different activated carbon adsorbents.

Agricultural adsorbents	CO_2 capture capacity (mmol CO_2/g)	Conditions	References
Commercial activated carbon	2.10	100% CO_2, 298 K, 1.0 bar	[24]
Coffee grounds activated carbon	4.80	100% CO_2, 273 K, 1.0 bar	[25]
	3.00	100% CO_2, 298 K, 1.0 bar	
Almond shell activated carbon	2.70	100% CO_2, 298 K, 1.2 bar	[26]
Olive stone activated carbon	3.10	100% CO_2, 298 K, 1.2 bar	[26]
Palm kernel char (PKC)	1.14	100% CO_2, 303 K, 1.0 bar	[27]
	1.71	100% CO_2, 303 K, 1.5 bar	
	2.13	100% CO_2, 303 K, 2.0 bar	
	5.60	100% CO_2, 303 K, 4.0 bar	
Palm activated char (PAC)	1.66	100% CO_2, 303 K, 1.0 bar	[27]
	2.88	100% CO_2, 303 K, 1.5 bar	
	3.87	100% CO_2, 303 K, 2.0 bar	
	7.32	100% CO_2, 303 K, 4.0 bar	
African palm shell	6.30	100% CO_2, 273 K, 1.0 bar	[28]
	4.40	100% CO_2, 298 K, 1.0 bar	
MMEA–Palm shell activated carbon	1.00	Equimolar of amines	[29]
AMP–Palm shell activated carbon	1.50	Equimolar of amines	[29]
Coconut shell activated carbon	5.60	100% CO_2, 273 K, 1.0 bar	[28–30]
	3.90	100% CO_2, 298 K, 1.0 bar	
	3.70	100% CO_2, 273 K, 1.0 bar	
Activated coconut modified with Cu/Ce	0.24	100% CO_2, 298 K, 1.0 bar	[31]
Poplar anthers KOH–activated carbon	3.45	100% CO_2, 298 K, 1.0 bar	[32]
Bagasse impregnated with $ZnCl_2$ and carbonized	1.82	100% CO_2, 303 K, 1.0 bar	[33]
Ammonia treated activated carbon	1.70	100% CO_2, 298 K, 1.0 bar	[34]
Bean dreg nitrogen enriched activated carbon	4.24	100% CO_2, 298 K, 1.0 bar	[35]
BPL–activated carbon	7.00	100% CO_2, 298 K, 35 bar	[36]
MAXSORB–activated carbon	25.00	100% CO_2, 298 K, 35 bar	[36]
Fly ash activated carbon	0.27	16% CO2, 298 K, 1.0 bar	[37]
Fly ash–Na_2SO_3	2.25	16% CO2, 298 K, 1.0 bar	[37]

Other researchers also have reported that adsorbent originated from biomass is very effective to be used as it works well under wide range of temperatures and humidity levels, inert and safe to handle, easily accessible and cost-effective [38–41]. In this study, kenaf (*Hibiscus cannabinus L.)* was chosen as adsorbent for CO2 separation study. Kenaf is grown in Peninsular Malaysia, and is known to be renewable resources, low plantation cost, short period of maturity, and biodegradable [42]. Inagaki et al. [43] revealed that kenaf core has high possibility to produce surface area as high as 3000 m^2/g and very large micro–pores volumes of about 1 mL/g. Moreover, results obtained via scanning electron microscopy (SEM) has identified that kenaf core is composed of porous structure with the primary and minor pore structures forming the interconnected pore structures [44]. The application of kenaf core as adsorbent has been reported for water treatments [45–49], bioremediation treatments [50], oil treatments [46,51,52] animal bedding materials [47] and CO_2 adsorption using carbonaceous kenaf [41].

Several studies have been conducted on modified kenaf after chemical treatment process. It was reported that the adsorption of metal cations (adsorbates) onto/into the lignocellulosic fibers depends on the ionizable characteristics of the cellulosic functional groups such as carboxylic and phenolic groups [53,54]. Mahmoud et al. [55] have found that treatment of kenaf core fiber with HCl increased the BET surface area and hence improved the adsorption of methylene blue dye. Sajab et al. [49] also reported that the chemically modified kenaf core in a presence of citric acid has higher the adsorption capacity towards methylene blue than the raw kenaf. Moreover, $ZnCl_2$ was used as a carbonizing promoter for kenaf in the treatment of oil and heavy–metal contamination [46]. Othman and Akil [41] also used $ZnCl_2$ as a promoter for carbonaceous kenaf in CO_2 adsorption study.

In other CO_2 separation studies, the impregnation of amine on adsorbent surfaces was able to enhance the adsorption capacity for different types of adsorbents (MCM-41, mesoporous silica and silica) [56,57,58]. Therefore, with the abundance of kenaf grown in Penisular Malaysia, various studies are needed to explore the potential of kenaf as agro-based adsorbent. With specific modification, the adsorption capacity may increase since there is a strong interaction between the adsorbate and the adsorbent. Therefore this paper presents the performance of kenaf as CO_2 adsorbent after amine modification.

In principle, the adsorption of CO_2 on amine–functionalized adsorbent involves chemical interaction between basic active amine sites (adsorbent) and CO_2 adsorbates. The reaction would produce ammonium carbamate (Eq. (1)) in anhydrous condition and ammonium bicarbonate (Eq. (2)) inhydrous condition [59,60]. Based on those reaction, 1 mol of CO_2 reacts with 2 mol amine groups bound on surface to produce 1 mol of carbamate, in the absence of water. Otherwise, in the presence of water, 1 mol CO_2 reacts with 1 mol surface–bound amine group, resulting ammonium bicarbonate that would improves the CO_2 adsorption capacity.

$$CO_2 + 2R\text{–}NH_2 \leftrightarrow RNH_3^+ + RNHCO_2^- \quad (1)$$

$$CO_2 + R\text{–}NH_2 \leftrightarrow R\text{–}NH_3^+HCO_3^- \quad (2)$$

This paper presents the performance of modified kenaf core as CO_2 adsorbent. In order to enhance the adsorption capacity, kenaf was functionalized using different type of amines (primary, secondary, and tertiary amines). Adsorption and regeneration study of selected amine-modified kenaf was conducted in a pressure swing adsorption (PSA) system.

2. Material and methods

In this study, kenaf inner core obtained from National Kenaf and Tobacco Board (NKTB), Pasir Putih, Kelantan was selected as a main precursor. The amines used for functionalization of kenaf are Monoethanolamine (MEA), Diethanolamine (DEA), Methyldiethanolamine (MDEA), 2–Amino–2–Methyl–1–Propanol (AMP), Polyethyleneimine (PEI), Diethylenetriamine (DETA), Triethylenetetramine (TETA), Tetraethylenepentamine (TEPA), Diisopropylamine (DIPA), Pentaethylenehexamine (PEHA), Triethanolamine (TEA), and Diglycolamine (DGA). Methanol was used as a solvent during the functionalization process. The gases involved are carbon dioxide (CO_2, 99.999% purity), nitrogen (N_2, 99.999% purity), and helium (He, 99.999%

purity), and were supplied by Mega Mount Industrial Gases Sdn. Bhd.

2.1. Amine wetness impregnation method

The functionalization of amines on kenaf was carried out via a conventional technique known as incipient wetness impregnation method as reported by Chatti et al. [60]. The wetness impregnation procedure was started by mixing a dried kenaf core in methanol solvent in a solid to liquid ratio of 1:20 (by weight). This procedure was conducted in two stages prior to separation and air–drying. In different container, alcoholic amine solution was prepared by mixing amine with methanol and stirred for 20 min. After that, the kenaf was added into the alcoholic amine solution and stirred for 15 min. The initial amine concentration used is 50 wt%. Then, the mixture was agitated for 5 h for impregnation with agitation rates of 600 rpm. Finally, the amine–-functionalized kenaf was filtered and dried, while the alcoholic amine solution was collected for pH analysis.

2.2. Characterization

The kenaf samples were subjected to several characterization techniques. The surfaces morphology of amine–functionalized kenaf samples were characterized under electron microscopic analysis using Field Emission Scanning Electrons Microscope (FESEM). The sample specimen was sputter coated with the thin layer of gold metal in order to provide appropriate surface condition, to avoid electrostatic surface charging, and to protect samples from thermal damage by the electron beam during the analysis. The elemental composition of amine-modified kenaf was determined by Electron Dispersive X-ray spectrocopy (EDX).

Identification of chemical bond functional groups by their characteristic absorption of infrared radiation was conducted out using Fourier Transforms Infrared (FTIR) spectroscopy. Initially, the sample was milled with potassium bromide (KBr) in a ratio of 1:100 for sample to KBr. After that, the mixture was pressed using a hydraulic press (Carver Hydraulic Unit Model 3912) under a pressure of 5 t. The IR vibration spectrums were collected for 10 scans and recorded in a mid–infrared region of 4000–370 cm^{-1} with 400 cm^{-1} resolution.

2.3. CO_2 adsorption and regeneration study

The CO_2 adsorption study was conducted in pressure swing adsorption (PSA) unit (Fig. 1). The column has a diameter and height dimension of 1 cm and 15 cm, respectively. The amine functionalised adsorbent was placed at the centre of column with the bed height of 4 cm. A molecular sieve was placed at the top and bottom of adsorbent bed to adsorb moisture in the feed stream. A glass wool was placed in the column to fix the position of adsorbent in the column. The PSA operation was conducted based on Skarstrom cyclical manner that involves four sequential steps that are pressurization, adsorption, blown down and purging [61]. In this adsorption-desorption study, the flow rate of CO_2 enter the adsorption column was set at 300 cm^3/s until the column reached a pressure of 1.5 bar. Then, CO_2 was retained in the column for 5 min to allow for adsorption. After that, CO_2 that not adsorb were blown down to the adjacent column and was retained for another 5 min. After 5 min, CO_2 was blown down as "raffinate gas" and the amount of gas leaving the column was determined using gas chromatography (GC). To regenerate the adsorbent, nitrogen gas (N_2) was passed through the highly–CO_2–loaded adsorbent bed for desorption at gauge pressure of 1.01325 bar. During this process, the "extract gases" were removed in counter-current flow of direction for an hour. The gas stream composition was analysed using GC analyser for complete CO_2 removal. These steps is a one-cycle operation (adsorption-desorption). The regeneration study was conducted for 10 consecutive cycles of operations.

3. Results and discussions

3.1. Characterization

In this study, the morphologies of kenaf after the functionalization with various types of amines were observed under Field Emission Scanning Electron Microscope (FESEM) as presented in Fig. 2.

The FESEM morphology shows that the impregnation of amines affected the kenaf structure. Some surfaces are full of cavities, others showed fragmented and rupture of the pores. Serrated and uneven ridge surfaces leads to partially blocked pores. Based on the FESEM micrographs, the impregnation of amines on kenaf resulted in a significant effect on the pore structure and surface of kenaf.

The IR spectra was analysed to determine the functional groups exist in the sample. In this analysis, kenaf sample was impregnated with different type of amines with the weight ratio of 50% and were subjected to the FTIR analysis. The scanning IR spectra of each sample are shown in Fig. 3.

Based on the IR spectra, the amine–functionalized kenaf samples do not show any significant differences. This is probably due to low amine loading used in the impregnation process. The IR spectra shows the broad bands within a range of 3600–3200 cm^{-1} for all the amine-

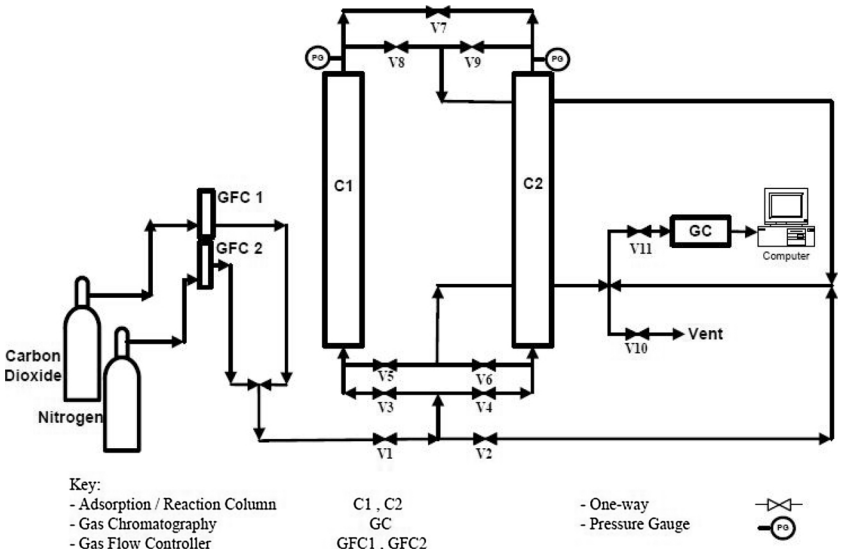

Fig. 1. Schematic diagram of dual–column PSA experimental unit.

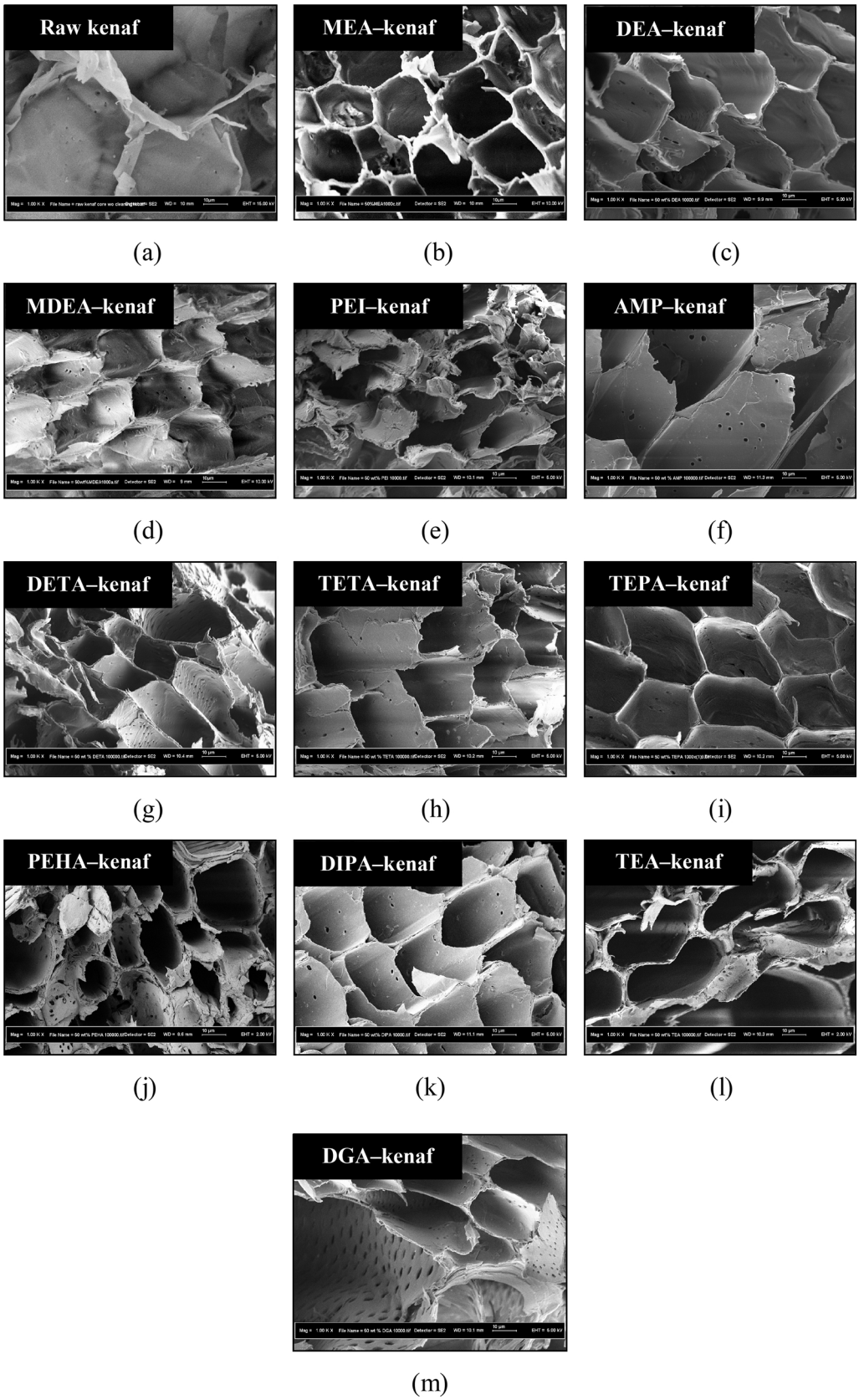

Fig. 2. FESEM microscopy of amine–-functionalized kenaf.

functionalized kenaf samples represents hydrogen bond linkages (−OH) of cellulose in raw kenaf. But, the absence of peaks at band position of 2861 cm^{-1} for the amine–functionalized kenaf samples indicates the shifted of the stretching aliphatic alkyl groups (−CH_2 and/or −CH_3) in the cellulose. The elimination of peaks at band position of 1725 cm^{-1} after the impregnation of MEA, DEA, MDEA, AMP, TETA, TEPA, PEHA,

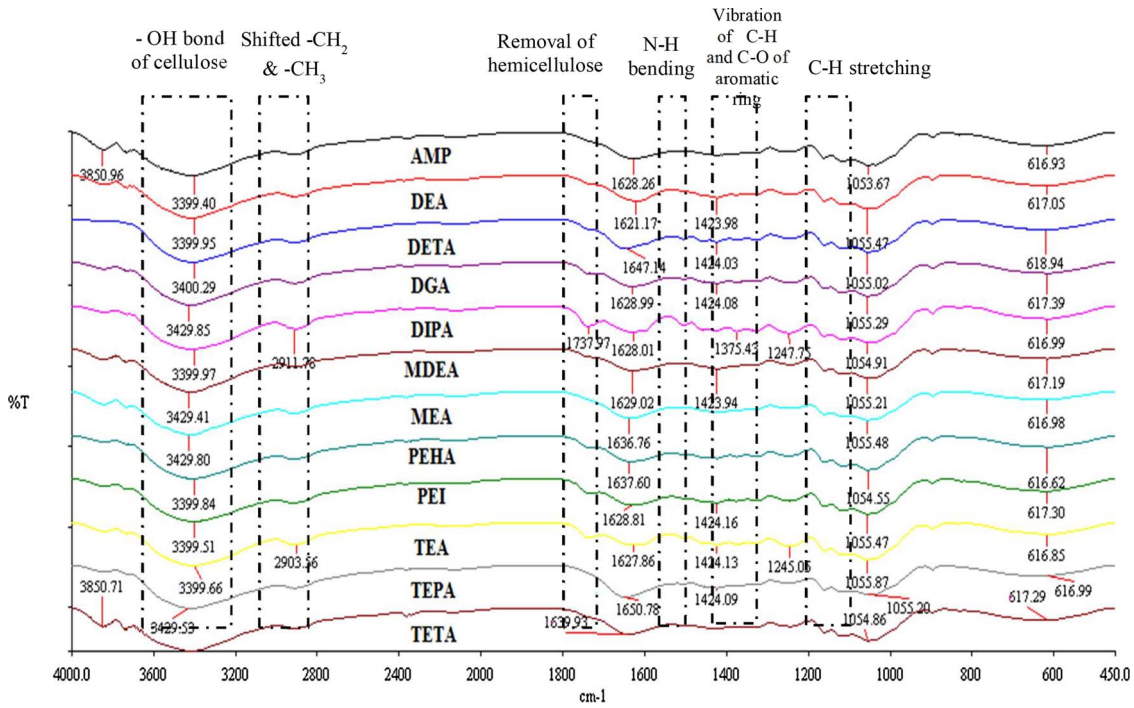

Fig. 3. IR spectra of various types of amine–functionalized kenaf samples.

DETA, and DGA on kenaf indicates that those amine functional groups are proficient in removing the hemicellulose of kenaf. Gibson [62] also concluded that the modification removes the amorphous hemicellulose of kenaf. Then, the impregnation of MEA and AMP also eliminates the peak at 1377 cm^{-1} due to the bending of C—H and C—O of aromatic rings in polysaccharides. The existence of peaks around 1550–1450 cm^{-1} for PEI, DETA, TEPA, PEHA, DIPA, DGA and TEA functionalized kenaf samples are attributed to the vibration of N—H bending. Besides, the peaks are also exist in the range of 1350–1000 cm^{-1} for PEI, DETA, PEHA, TEPA, DIPA, and TEA functionalized kenaf samples that denotes a C—N stretching in aliphatic amine groups. The determination of IR spectra in the amine–functionalized kenaf confirmed the presence of amine functional groups on kenaf surfaces.

3.2. Nitrogen content

The nitrogen content of amine-functionalized kenaf samples were determined using Energy Dispersive X–ray Spectroscopy (EDX). The elemental content of nitrogen indicates the extend of basicity characteristic of amine–functionalized kenaf samples. Raw kenaf sample was also accounted in this analysis as a comparison. The analysis was conducted for the kenaf samples with 50 wt% of amine loaded by wet impregnation method. Based on the elemental composition data, carbon (C), oxygen (O) and nitrogen (N) are the major elements present the samples. Table 2 shows the ratio of C, O and N content in kenaf. The nitrogen element in amine–functionalized kenaf sample indicates the basicity characteristic of the prepared sample.

In principle, the impregnation of amine on kenaf provides a basic active sites on the adsorbent surface that is essential for the adsorption of CO_2. However, the degree of basicity of amine–based adsorbent depends on the type of amine used since different type of amine have different percentages of nitrogen content. As indicated in Table 2, TEPA and PEHA functionalized on kenaf are amongst the highest nitrogen content as compared to other amine–functionalized kenaf adsorbents. This is due to the high nitrogen element attached on the main ligands of each amine group. TEPA and PEHA amines are composed of five and six nitrogen elements respectively, attached on its main ligand that induces high percentage of nitrogen content (as computed by EDX). Based on this analysis, TEPA and PEHA amines may contribute to higher basicity than other types of amines.

Table 2
Elemental ratio of carbon (C), oxygen (O) and nitrogen (N) in kenaf samples.

Sample	Elemental ratio		
	Carbon (C)	Oxygen (O)	Nitrogen (N)
Raw kenaf	1.04	1	–
MEA–kenaf	1.45	1	0.05
DEA–kenaf	1.56	1	0.01
MDEA–kenaf	1.15	1	0.07
PEI–kenaf	1.41	1	0.02
AMP–kenaf	1.43	1	0.13
DETA–kenaf	1.71	1	0.14
TETA–kenaf	2.36	1	0.21
TEPA–kenaf	2.21	1	0.25
PEHA–kenaf	1.66	1	0.20
DIPA–kenaf	1.11	1	0.15
TEA–kenaf	1.23	1	0.03
DGA–kenaf	1.39	1	0.03

3.3. Nitrogen adsorption isotherm

The surface area and pore size of raw kenaf and amine–functionalized kenaf samples were determined from nitrogen adsorption isotherm analysis at 77 K. The Brunauer Emmet Teller (BET) surface area was determined at a relative pressure between 0.0247 to 1. In this study, only MEA and TEPA functionalized kenaf were selected for the nitrogen adsorption isotherm analysis. MEA was chosen because it is extensively used in industry as absorbent. However, the selection of TEPA was based on sample with high nitrogen content that may contribute to high adsorption capacity. The nitrogen adsorption isotherms of raw kenaf, MEA–functionalized kenaf and TEPA–functionalized kenaf are presented in Figs. 4–6 respectively. The adsorption isotherm of raw kenaf core obeyed Type II of IUPAC classification isotherm that indicates the macroporous structure of kenaf core with the monolayer

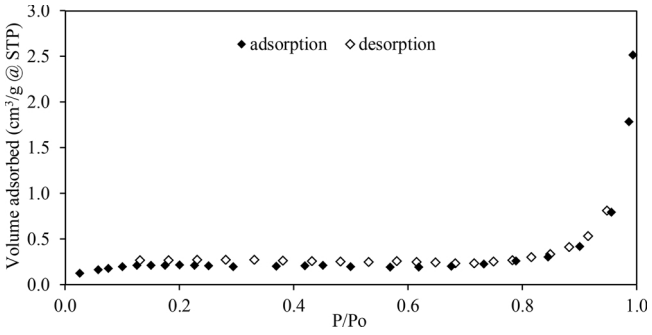

Fig. 4. N_2 adsorption–desorption isotherm of raw kenaf core.

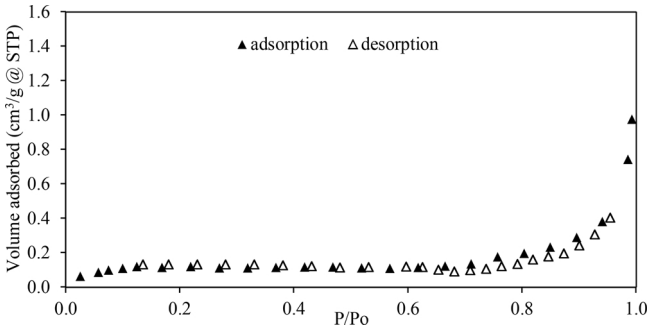

Fig. 5. N_2 adsorption–desorption isotherm of MEA–functionalized kenaf.

and multilayer adsorptions. There are two increments exist; the first increment occurred at very low relative pressure of P/Po < 0.10 that ascribed for a freely penetration of N_2 molecules into the macroporous structures without steric factor. However, the abrupt increment of nitrogen adsorption isotherm at high relative pressure (P/Po > 0.90) is attributed to the multilayer adsorption and capillary condensation of N_2 onto kenaf pores.

Figs. 5 and 6 present the nitrogen (N_2) adsorption–desorption isotherms of amine–functionalized kenaf adsorbents at temperature of 77 K. Based on the graphs, the nitrogen isotherm for MEA and TEPA modified kenaf are also classified into Type II of the BDDT adsorption isotherm classification. The adsorption isotherm showed that the pore structure of amine–functionalized kenaf has macroporous formation and has a tendency towards the monolayer and multilayer adsorption. The two increments are identified at low and high relative pressure range. The first increment at low relative pressure (P/Po < 0.1) is attributed to the gas adsorption phenomenon of macroporous amine–-functionalized kenaf adsorbent, a freely penetration without affected by steric factor. However, a steep increment of nitrogen adsorption isotherm appears at relative pressure (P/Po) higher than 0.84 for MEA and

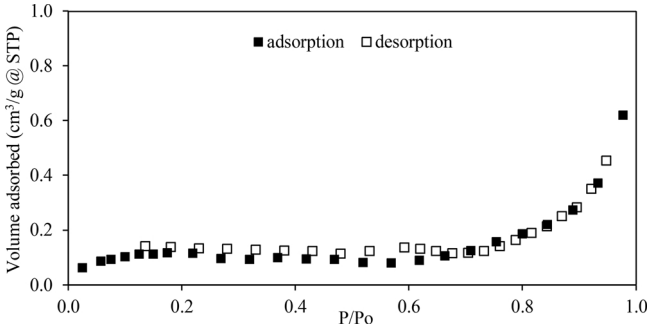

Fig. 6. N_2 adsorption–desorption isotherm of TEPA–functionalized kenaf.

Table 3
Physical textural properties of raw kenaf and amine–functionalized kenaf.

Sample	BET surface area (m^2/g)	Micropores volume (cm^3/g)	Average pore diameter (Å)
Raw kenaf	0.769 ± 0.0285	0.000322	88.50
MEA–kenaf	0.438 ± 0.0236	0.000156	81.12
TEPA–kenaf	0.431 ± 0.0178	0.000156	81.50

TEPA functionalized kenaf adsorbent represents a multilayer adsorption and/or capillary condensation of nitrogen molecules penetrating into the adsorbent surfaces. These results show that raw kenaf has relatively higher nitrogen adsorption than amine–functionalized kenaf.

Based on the nitrogen adsorption isotherm, BET surface area, pore volume, and average pore diameter of the samples are summarized in Table 3. The result is in line with the study conducted by Sajab et al. [48] who has reported a low BET surface area of kenaf core (as low as 0.810 m^2/g). Then, the functionalization of amine on kenaf surface has reduced available surface for N_2 adsorption; hence reduce the volume of N_2 adsorbed and resulted to a lower BET surface area and micropore volume than the raw kenaf. It is because the dispersion of amine occurs within the structure of kenaf after the impregnation process. However, the BET surface area and average pore diameter of MEA-functionalized kenaf is slightly higher than TEPA-functionalized kenaf. In general, the functionalization (via impregnation technique) of amines has affected the physical properties of kenaf structure.

3.4. CO_2 adsorption

The CO_2 adsorption on kenaf adsorbent was conducted in a pressure swing adsorption system (PSA). In this study, the effect of different types of amines and effect of amine loading were evaluated. The performance of amine-functionalized kenaf was evaluated using single column adsorption.

3.4.1. Effect of different types of amines

Modification of kenaf was conducted using different amine–-functionalized groups (MEA, DEA, MDEA, AMP, PEI, DETA, TETA, TEPA, DIPA, PEHA, TEA, and DGA). The CO_2 capture capacity of each amine–functionalized kenaf sample was carried out in a single–bed column at a pressure of 1.5 bar with feed flowing rate of 300 cm^3/min. The amount of CO_2 adsorbed are shown in Fig. 7.

The impregnation of TEPA on kenaf achieved the highest adsorption capacity with the value of 0.914 mmol/g. Other samples also show higher adsorption capacity than raw kenaf. The results elucidate that the presence of amine (nitrogen-rich) on kenaf surface adsorbent induces higher CO_2 adsorption. Table 4 shows a comparison on different class of amines. Based on the results, TEPA that consist of primary and

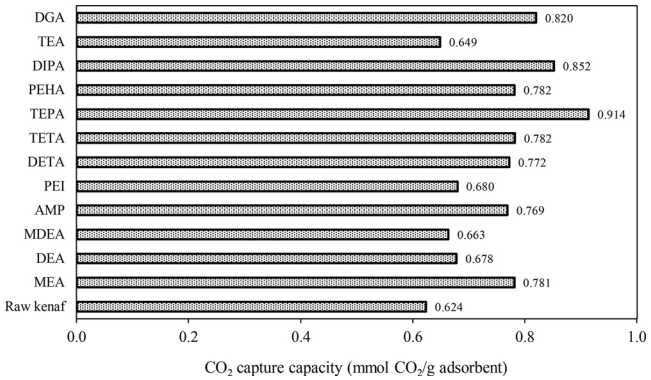

Fig. 7. CO_2 adsorption capacity of raw kenaf and amine–functionalized kenaf.

Table 4
CO_2 capture capacity for amine–functionalized kenaf sample.

Class of amine	Amine	CO_2 capture capacity (mmol/g)
Primary amine (1°)	Monoethanolamine (MEA)	0.781
	Amino–Methyl–Propanol (AMP)	0.769
	Diglycolamine (DGA)	0.820
Secondary amine (2°)	Diethanolamine (DEA)	0.678
	Polyethyleneimine (PEI)	0.680
	Diisopropylamine (DIPA)	0.852
Tertiary amine (3°)	Methyldiethanolamine (MDEA)	0.663
	Triethanolamine (TEA)	0.649
Combination of Primary/ Secondary (1°/2°)	Diethylenetriamine (DETA)	0.772
	Triethylenetetramine (TETA)	0.782
	Tetraethylenepentamine (TEPA)	0.914
	Pentaethylenehexamine (PEHA)	0.782

Table 5
pH value and CO_2 adsorption capacity of amine–functionalized kenaf.

Sample	pH of amine solution	CO_2 adsorption capacity (mmol/g)
TEPA–kenaf	10.82	0.914
PEHA–kenaf	10.81	0.782
DIPA–kenaf	10.76	0.852
DETA–kenaf	10.74	0.772
AMP–kenaf	10.62	0.769
MEA–kenaf	10.60	0.781
TETA–kenaf	10.43	0.782
DGA–kenaf	10.40	0.820
PEI–kenaf	10.31	0.680
DEA–kenaf	10.24	0.678
MDEA–kenaf	9.58	0.663
TEA–kenaf	9.37	0.649

secondary amines present the highest CO_2 capture capacity. In contrast, modification of kenaf using tertiary amines show a less amount of CO_2 adsorption capacity.

The reaction of primary and secondary amines with CO_2 are represented by Eqs. (3) and (4), respectively. Eq. (5) is the overall reaction for primary and secondary amine, and Eq. (6) represents reaction for tertiary amine [17,63–66].

$$RR'NH + CO_2 \leftrightarrow RR'NH^+COO^- \text{ (Zwitterion)} \quad (3)$$

$$RR'NH^+COO^- + RR'NH \leftrightarrow \underset{\text{(Carbamate ion)}}{RR'NCOO^-} + RR'NH_2 \quad (4)$$

Eq. (5) is the overall reaction for primary and secondary amines with CO_2 molecule.

$$\underset{\text{(Amine)}}{2RR'NH} + CO_2 \leftrightarrow \underset{\text{(Carbamate ion)}}{RR'NCOO^-} + \underset{\text{(Ammonium ion)}}{RR'NH_2^+} \quad (5)$$

The reactions of primary and secondary amines with CO_2 occur in two stages. At the first stage, a reaction of one mole of amine with one mole of CO_2 yields of zwitterion (Eq. (3)), while second reaction occurs between the intermediate zwitterion with other one mole of amine to produce carbamate molecule (Eq. (4)). Eq. (5) is the overall reaction of amine molecules with CO_2 molecule in which two moles of amines are required for each CO_2 molecule. However, the absence of hydrogen ions (H^+) in the tertiary amine resulted to the formation of bicarbonate compound as the reaction between amine with CO_2 molecule as represented by Eq. (6).

$$\underset{\text{(Carbamate ion)}}{RR'NCOO^-} + H_2O \leftrightarrow \underset{\text{(Free amine)}}{RR'NH} + \underset{\text{Biocarbonate ion}}{HCO_3^-} \quad (6)$$

where R = C_2H_4OH

Based on the reaction, the direct reaction of primary and secondary amines with CO_2 molecule will produce carbamate ion ($RR'NCOO^-$). The production of carbamate ion leads to the faster CO_2 capture kinetics [24]. The reaction follows the stoichiometric ratio of amine to CO_2 of 2:1. Since the tertiary amine does not produce carbamate ion as immediate as primary and secondary amines, the CO_2 adsorption capacity are relatively lower than the primary and secondary amines. The results also shows that the binary amine group (consists of primary and secondary class) have higher CO_2 adsorption capacity than a single class of amine.

The combination of primary class ($–NH_2$) and secondary class (–NH) of amines give more advantages for the impregnation on kenaf than a single class of amine, as shown by the adsorption capacity of TEPA. TEPA that comprised of two groups of primary class and three groups of secondary class shows the highest CO_2 capture capacity with the value of 0.914 mmol/g. The presence of four methyl groups ($–CH_3$) in DIPA (CO_2 capture capacity of 0.852 mmol/g) also improved the basicity characteristic that give advantages for the CO_2 adsorption. It is because the methyl group would stabilize the ammonium ion; hence improve the CO_2 capture capacity of DIPA. For the primary amine group, MEA and DGA show higher CO_2 adsorption capacity than AMP. It is expected that steric character of AMP reduces the stability of the carbamates, thus reduces the CO_2 capture capacity. Similarly, sterically hindered in MDEA and TEA induces low CO_2 capture capacity.

The basicity of amine–functionalized kenaf adsorbent was examined to determine its effect on gas adsorption. In principle, the impregnation of amine on the surface of kenaf promotes the basic active sites that would facilitate the interaction towards acidic CO_2 molecules via the

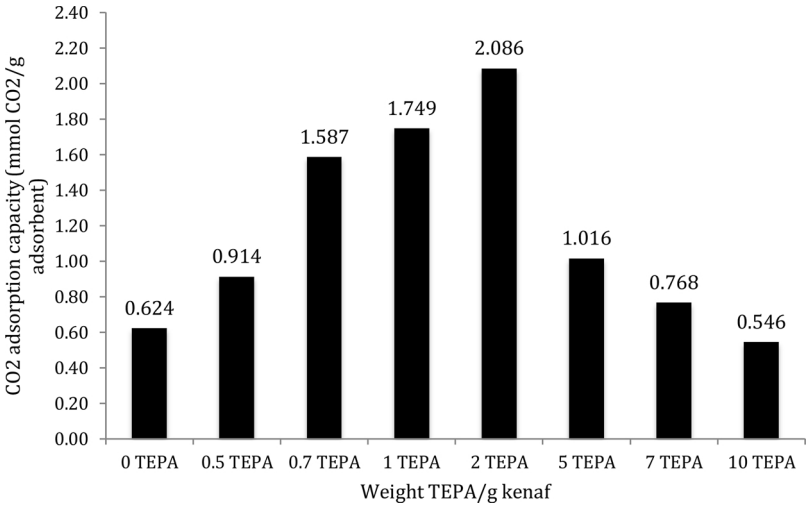

Fig. 8. CO_2 adsorption capacity of TEPA–functionalized kenaf at different loadings.

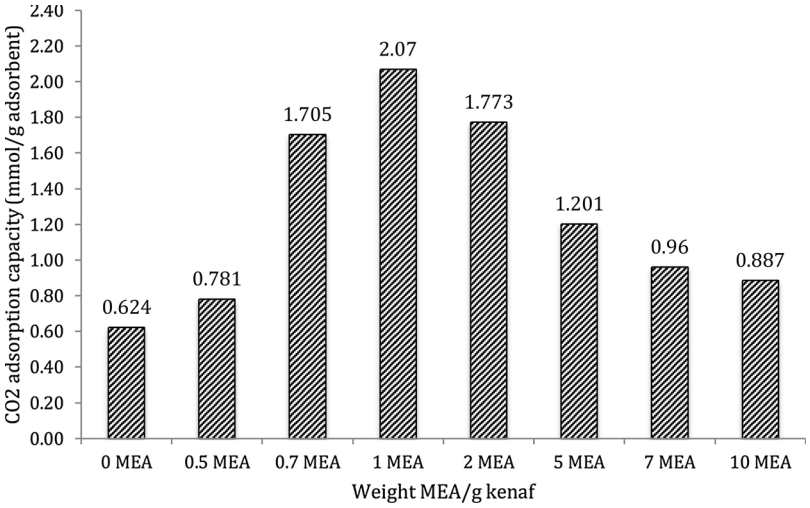

Fig. 9. CO_2 adsorption capacity of MEA–functionalized kenaf at different loadings.

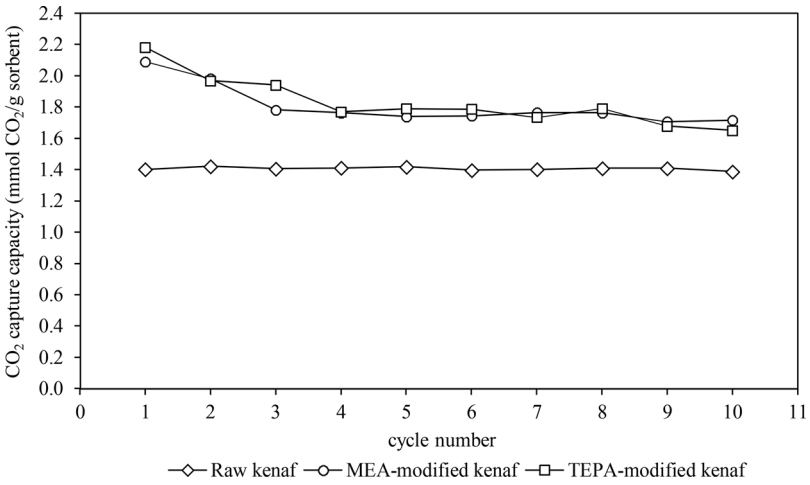

Fig. 10. Adsorption capacity of kenaf samples for 10 cyclic operation.

formation of the polarized covalent bond. As a result, the acidic-basic interaction could improve the CO_2 adsorption capacity. Chatti et al. [31] also reported that the amine active sites available on the porous adsorbent surface improved the CO_2 adsorption capacity. Table 5 shows the pH value and the amount of CO_2 adsorbed on amine functionalised kenaf.

As shown in Table 5, all kenaf samples have basic character since the pH of amine used are more than 7. TEPA and PEHA functionalized kenaf samples have almost the same pH value. More alkyl groups ($-CH_2$) exist in TEPA and PEHA able to stabilize the formation of ammonium ions; hence increases the basicity of amine that leads to high CO_2 adsorption. The alkyl groups and the amines have contributed to higher CO_2 adsorption. In contrast, the pH values of MDEA and TEA (tertiary amine) are amongst the lowest. Based on CO_2 adsorption capacity, TEPA–functionalized kenaf sample was selected for further investigation together with MEA–functionalized kenaf sample. MEA–-functionalized kenaf was also selected because it is commonly used in CO_2 removal process.

3.4.2. Effect of amine loadings

The amine loading is also a factor that affects the physical and structural characteristic of kenaf which then affects the amount of CO_2 adsorbed. Therefore, the effect of amine loading was investigated by varying the weight ratio of amine to kenaf between 0.5 to 10. The CO_2 adsorption capacity study was conducted in a single–column system at pressure of 1.5 bar with feed flowing rate of 300 cm^3/min. The CO_2 adsorption capacity of TEPA and MEA functionalised kenaf at different amine loading are shown in Figs. 8 and 9, respectively.

Table 6
Percentage of regeneration for kenaf samples.

Sample	CO_2 capacity at 1st cycle (mmol CO_2/g)	CO_2 capacity at 10th cycle (mmol CO_2/g)	Regeneration (%)
Raw kenaf	1.401	1.388	99.07
MEA–modified kenaf	2.090	1.717	82.15
TEPA–modified kenaf	2.182	1.650	75.62

As shown in Figs. 8 and 9, the amount of amine loaded onto kenaf influence the CO_2 adsorption capacity. For TEPA, the highest CO_2 adsorption capacity (2.086 mmol/g) is in the ratio of 2:1 (TEPA:kenaf). The highest CO_2 adsorption for MEA-kenaf is 2.070 mmol CO_2/g in the ratio of 1:1 (MEA:kenaf). The balance between the nitrogen content and available surface area were investigated by varying the ratio of amine and kenaf. At higher amine content, the structure were ruptured, thus affects the CO_2 adsorption. Although high amine loading gives high percentage of nitrogen content, but the destruction of kenaf structure may also reduce the available surface area for CO_2 adsorption. Thus,

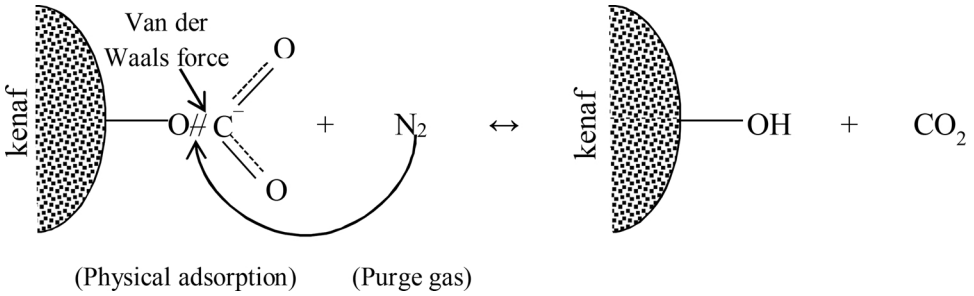

Fig. 11. Proposed desorption (regeneration) mechanism of raw kenaf.

this study has suggested that the suitable ratios for TEPA and MEA impregnated on kenaf surface are 2:1 and 1:1, respectively.

3.5. Regeneration

In addition to high adsorption capacity, good adsorbents must have a stable adsorption performance in cyclic operations. Regeneration is an essential factor that should to be considered for the selection of good adsorbent. This study shows the regeneration performance of kenaf and amine–functionalized kenaf samples. It was conducted for ten (10) consecutive cycles of operations and each cycle involves adsorption and desorption requires 60 min of operation. Fig. 10 shows the adsorption capacity for each cycle and the percentage of regeneration is shown in Table 6. The percentage of regeneration was calculated based on the CO_2 adsorption capacity at the tenth (10th) to the first (1st) cycle operation as reported by Lee et al. [29]

As shown in Fig. 10, raw kenaf presents sustainable adsorption performance for ten (10) consecutive cycles of operations. The interaction of CO_2 with the surface of raw kenaf is a physical adsorption involving of weak intermolecular forces (Van de Waals forces). Due to the weak intermolecular forces, this physisorption interaction does not need a significant change in the electronic orbital pattern for each species. As a result, the CO_2 (sorbate) has a high tendency to move freely over the kenaf surfaces (sorbent). The adsorbed CO_2 molecules do not fix to any particular sites on the solid surface. Thus, the energy required to break the weak interaction force is low. The adsorbed molecule can be removed (desorbed) to almost the same amount, as indicates by high regeneration value of raw kenaf (99.07%). Fig. 11 shows the proposed mechanism for the desorption process step of the raw kenaf.

For MEA and TEPA functionalized kenaf samples, a rapid reduction in the first three cycles of operations is due to chemisorption mechanism, a chemical reaction between amine on kenaf surface (adsorbent) with CO_2 molecule (adsorbate). Based on Eq. (4), the chemical reaction would produce carbamate molecules. As the chemical reaction occured, CO_2 molecule would be chemically bonded to the surface of amine–functionalized kenaf by forming carbamate molecules, attached via a strong covalent bond and occupying the specific adsorption sites. The energy required to desorb (in the form of carbamate molecule) from the amine-functionalized kenaf surface is relatively higher than the raw kenaf (only involves Van der Waals' force). It is due to the presence of orbital overlap and charge transfer in the chemical adsorption that causes the carbamates not easily to be removed from the adsorbent during desorption process [29,67]. This condition explained low regeneration values obtained by MEA–functionalized kenaf (82.15%) and TEPA–functionalized kenaf (75.62%). This study also shows that the regeneration values decrease when the strength of adsorbate-adsorbent is increased. The proposed desorption mechanism of CO_2 from the surface of amine–functionalized kenaf adsorbent is shown in Fig. 12.

Based on the experimental results obtained, the amine functional group serves as a basic active sites on the surface of kenaf and react with the CO_2 molecule. The basic active sites are depending on the amount of nitrogen elements (N) in the amine group. Since TEPA has the higher amount of nitrogen elements attached to the main ligand than MEA, the pH value is relatively higher that leads to the higher CO_2 adsorption capacity. Consequently, the energy needed to break the chemical bond (covalent bond) of TEPA is also relatively higher than MEA as indicated by the regeneration value of TEPA and MEA (Table 6). This study is in line with the research conducted by Lee et al. [29]. They have reported that the regeneration value decreased as the energy needed for desorption process increases. Fig. 10 also showed that the adsorption capacity from the fourth (4th) to the tenth (10th) cycle are relatively constant. This phenomenon proved that the physisorption are also take place on the adsorption sites. It is proposed that the chemisorption and physisorption processes are occurred simultaneously on the amine–functionalized kenaf adsorbent surface. The regeneration study showed that regeneration is more effective for raw kenaf than amine–functionalized kenaf adsorbent.

4. Conclusions

This study proved that kenaf is another potential material for CO_2 adsorbent. The impregnation of amine on the kenaf surface has improved the adsorptive characteristic of kenaf adsorbent. At the weight ratio of 0.5:1, TEPA showed the high CO_2 adsorption capacity (0.914 mmol/g). However, the adsorption capacity was improved by increasing the amount of amine loaded on the kenaf. Thus, it was found that the highest amount of CO_2 adsorbed is 2.07 mmol/g of MEA-modified kenaf at the ratio of 1:1 and 2.08 mmol of CO_2 adsorbed on TEPA-modified kenaf at a ratio of 2:1. The regeneration study showed that CO_2 can easily being removed from the raw kenaf, regeneration

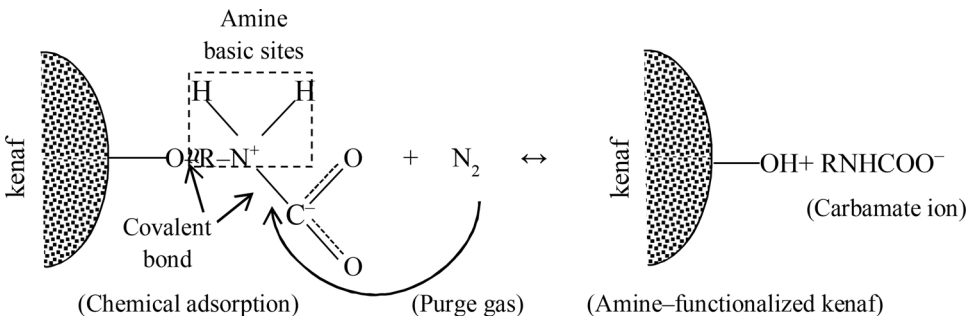

Fig. 12. Proposed desorption mechanism of amine–functionalized kenaf.

value (99.07%) higher than MEA–functionalized kenaf (82.15%) and TEPA–functionalized kenaf (75.62%). This is due to different mechanism of adsorption (physisorption and chemisorption) of CO_2 on kenaf adsorbent.

Acknowledgements

This work was supported by Ministry of Science, Technology and Innovation (Grant No: 06-01-06-SF1062), Ministry of Education (MyBrain15 scholarship awarded to Nabilah Zaini) and Universiti Teknologi Malaysia. We also acknowledged the material (kenaf) supplied by National Kenaf and Tobacco Board (NKTB), Kelantan, Malaysia.

References

[1] M. Castro, D. Gómez-Díaz, J.M. Navaza, Carbon dioxide chemical absorption using methylpiperidines aqueous solutions, Fuel 197 (2017) 194–200.
[2] M. Mehrpooya, R. Esfilar, S.M.A. Moosavian, Introducing a novel air separation process based on cold energy recovery of LNG intergrated with coal gasification, transcritical carbon dioxide power cycle and cryogenic CO2 capture, J. Clean. Prod. 142 (2017) 1749–1764.
[3] R. Augelletti, M. Conti, M.C. Annesini, Pressure swing adsorption for biogas upgrading. a new process configuration for the separation of biomethane and carbon dioxide, J. Clean. Prod. 140 (2017) 1390–1398.
[4] G. Hu, N.J. Nicholas, K.H. Smith, K.A. Mumford, S.E. Kentish, G.W. Stevens, Carbon dioxide absorption into promoted potassium carbonate solutions: a review, Int. J. Greenhouse Gas Control 53 (2016) 28–40.
[5] A. Ali, K. Maqsood, A. Redza, K. Hii, A.B.M. Shariff, S. Ganguly, Performance enhancement using multiple cryogenic desiblimation based pipeline network during dehydration and carbon capture from natural gas, Chem. Eng. Res. Des. 109 (2016) 519–531.
[6] F.R.H. Abdeen, M. Mel, M.S. Jami, S.I. Ihsan, A.F. Ismail, A review of chemical absorption of carbon dioxide for biogas upgrading, Chin. J. Chem. Eng. 24 (2016) 693–702.
[7] E. Sjöberg, S. Barnes, D. Korelskiy, J. Hedlund, MFI membranes for separation of carbon dioxide from synthesis gas at high pressures, J. Membr. Sci. 486 (2015) 132–137.
[8] E. Privalova, S. Rasi, P. Maki-Arvela, CO2 capture from biogas: absorbent selection, RSC Adv. 3 (2013) 2979–2994.
[9] J. Davison, K. Thambimuthu, Technologies for capture of carbon dioxide, in: E.S. Rubin, D.W. Keith, C.F. Gilboy (Eds.), Greenhouse Gas Cont. Technol. Vol. 7 Elsevier Science Ltd., Oxford, 2005, pp. 3–13.
[10] A. Krzemień, A. Wieckol-Ryk, A. Smoliński, A. Koteras, L. Wiecław-Solny, Assessing the risk of corrosion in amine-based CO2 capture process, J. Loss Prev. Process 43 (2016) 189–197.
[11] K.L.S. Campbell, Y. Zhao, J.J. Hall, D.R. Williams, The effect of CO2 loaded amine solvents on the corrosion of a carbon steel stripper, Int. J. Greenhouse Gas Control 47 (2016) 376–385.
[12] Y.-C. Chiang, R.-S. Juang, Surface modification of carbonaceous materials for carbon dioxide adsorption: a review, J. Taiwan Inst. Chem. Eng. 71 (2017) 214–234.
[13] A. Manase, U. Musa, D.Y. Muibat, D.A. Olalekan, M.A. Ibrahim, S. Bilyaminu, Diethanolamine functionalized waste tea activated carbon for CO_2 adsorption, Inter. Conf. Chem. Environ. Bio. Sci. March 18–19. Dubai: CEBS, 2015, pp. 96–99.
[14] S. Choi, J.H. Drese, C.W. Jones, Adsorbent materials for carbon dioxide capture from large anthropogenic point sources, Chemsuschem 2 (2009) 796–854.
[15] M.G. Plaza, S. García, F. Rubiera, J.J. Pis, C. Pevida, Post–combustion CO2 capture with a commercial activated carbon: comparison of different regeneration strategies, Chem. Eng. J. 163 (2010) 41–47.
[16] A. Sayari, Y. Belmabkhout, R. Serna?Guerrero, Flue gas treatment via CO2 adsorption, Chem. Eng. J. 171 (2011) 760–774.
[17] C.H. Yu, C.H. Huang, C.S. Tan, A review of CO2 capture by absorption and adsorption, Aerosol Air Qual. Res. 12 (2012) 745–769.
[18] S.U. Rege, R.T. Yang, A novel FTIR method for studying mixed gas adsorption at low concentration: H_2O and CO_2 on NaX zeolite and γ-alumina, Chem. Eng. Sci. 56 (12) (2001) 3781–3796.
[19] B. Arstad, H. Fjellvag, K.O. Kongshaug, O. Swang, R. Blom, Amine–functionalized metal organic frameworks (MOFs) as adsorbents for carbon dioxide, Adsorption 14 (6) (2008) 755–762.
[20] M. Li, Dynamics of CO2 adsorption on sodium oxide promoted alumina in a packed–bed reactor, Chem. Eng. Sci. 66 (2011) 5938–5944.
[21] M.B. Yue, Y. Chun, Y. Cao, X. Dong, J.H. Zhu, CO2 capture by As–prepared SBA–15 with an occluded organic template, Adv. Funct. Mater. 16 (2006) (2006) 1717–1722.
[22] B. Spigarelli, S.K. Kawatra, An Approach to Carbon Dioxide Capture and Storage at Ambient Conditions: Laboratory Studies, Michigan Technological University, Houghton, 2012.
[23] Z.K. George, K. Margaritis, Green adsorbents for wastewaters: a critical review, Materials 7 (2014) 333–364.
[24] E.S. Kikkinides, R.T. Yang, S.H. Cho, Concentration and recovery of CO2 from flue gas by pressure swing adsorption, Ind. Eng. Chem. Res. 32 (1993) 2714–2720.
[25] M.G. Plaza, A.S. Gonzalez, C. Pevida, J.J. Pis, F. Rubiera, Valorisation of spent coffee grounds as CO2 adsorbents for post combustion capture applications, Appl. Energ. 99 (2012) 272–279.
[26] A.S. González, M.G. Plaza, F. Rubiera, C. Pevida, Sustainable biomass–based carbon adsorbents for post–combustion CO_2 capture, Chem. Eng. J. 230 (2013) 456–465.
[27] N.S. Nasri, U.D. Hamza, S.N. Ismail, M.M. Ahmed, R. Mohsin, Assessment of porous carbons derived from sustainable palm solid waste for carbon dioxide capture, J. Clean. Prod. 71 (2013) 148–157.
[28] A.S. Ello, K.C. Luiz, T. de Souza Albert, J. Mietek, Development of microporous carbons for CO_2 capture by KOH activation of african palm shells, J. CO_2 Util. 2 (2013) 35–38.
[29] C.S. Lee, Y.L. Ong, M.K. Aroua, W.M.A.W. Daud, Impregnation of palm shell based activated carbon with sterically hindered amines for CO_2 adsorption, Chem. Eng. J. 219 (2013) 558–564.
[30] D.D.P. Vargas, G.L. Giraldo, J.C. Moreno-Piraján, Enthalpic characterization of activated carbon monoliths obtained from lignocellulosic materials, J. Therm. Anal. Calorim. 111 (2013) (2013) 1067–1072.
[31] L. Fenrong, Y. Honghong, T. Xiaolong, N. Ping, Y. Qiongfen, K. Dongjuan, Adsorption of carbon dioxide by coconut activated carbon modified with Cu/Ce, J. Rare Earth 28 (2010) 334–337.
[32] J. Song, W. Shen, J. Wang, W. Fan, Superior carbon–based CO_2 adsorbents prepared from poplar anthers, Carbon 69 (2014) 255–263.
[33] A. Boonpoke, S. Chirakorn, N. Laosiripojana, S. Towprayon, Chidthaisong, Synthesis of activated carbon and MCM–41 from bagasse and rice husk and their carbon dioxide adsorption capacity, J. Sustain. Energy Environ. 2 (2011) 77–81.
[34] J. Przepiorski, M. Skrodzewicz, A.W. Morawski, High temperature ammonia treatment of activated carbon for enhancement of CO_2 adsorption, Appl. Surf. Sci. 225 (2004) 235–242.
[35] J. Qiao, Y. Liu, F. Hong, J. Zhang, A review of catalysts for the electroreduction of carbon dioxide to produce low–carbon fuels, Chem. Soc. Rev. 43 (2014) 631–675.
[36] A.H. Lu, G.P. Hao, X.Q. Zhang, Porous Materials for Carbon Dioxide Capture, Green Chemistry and Sustainable Technology, Springer-Verlag, Berlin Heidelberg, 2014, pp. 15–77.
[37] P. Brett, A. Spigarelli, Novel Approach to Carbon Dioxide Capture and Storage, Michigan Technological University, 2013 (Master Thesis).
[38] I. Anastopoulos, A. Bhatnagar, B.H. Hameed, Y.S. Ok, M. Omirou, A review on waste-derived adsorbents from sugar indystry for pollutant removal in water and wastewater, J. Mol. Liq. 40 (2017) 179–188.
[39] S. Rovani, M.T. Censi, SL, R. Cataluña, N. Fernandez, Development of a new adosrbent from agro-industrial waste and its potential use in endocrine disruptor compound removal, J. Hazard. Mater. 271 (2014) 311–320.
[40] N.S. Nasri, U.D. Hamza, S.N. Ismail, M.M. Ahmed, Assessment of porous carbons derived from sustainable palm solid waste for carbon dioxide capture, J Clean. Prod. 71 (2014) 148–157.
[41] M.R. Othman, H.M. Akil, The CO_2 adsorptive and regenerative behaviors of rhizopus oligosporus and carbonaceous hibiscus cannabinus exposed to thermal swings, Microporous Mesoporous Mater. 110 (2–3) (2008) 363–369.
[42] M.H.A. Basri, A. Abdu, N. Junejo, H.A. Hamid, K. Ahmed, Journey of kenaf in Malaysia: a review, Acad. J. 9 (11) (2014) 458–470.
[43] M. Inagaki, T. Nishikawa, K. Sakuratani, T. Katakura, H. Konno, E. Morozumi, Carbonization of kenaf to prepare highly–microporous carbon, Carbon 42 (2004) 890–893.
[44] M. Zaveri, Absorbency Characteristics of Kenaf Core Particles, North Carolina State University, 2004 (Master Thesis).
[45] K. Abe, Y. Ozaki, Wastewater treatment by using kenaf in paddy soil and effect of dissolved oxygen concentration on efficiency, Econ. Eng. 29 (2007) 125–132.
[46] M.R. Othman, H.M. Akil, J. Kim, Carbonaceous hibiscus cannabinus l for treatment of oil and metal contaminated water, Bioresour. Eng. J. 41 (2008) 171–174.
[47] S.J.J. Lips, G.M. Iniguez de Heredia, R.G.M. Op den Kamp, J.E.G. van Dam, Water absorption characteristics of kenaf core to use as bedding material, Ind. Crop. Prod. 29 (2009) 73–79.
[48] M.S. Sajab, C.H. Chia, S. Zakaria, S. Mohd Jani, P.S. Khiew, W.S. Chiu, Removal of copper (II) ions from aqueous solution using alkali–treated kenaf core fibers, Adsorpt. Sci. Technol. 28 (4) (2010) 377–386.
[49] M.S. Sajab, C.H. Chia, S. Zakaria, S.M. Jani, M.K. Ayob, K.L. Chee, P.S. Khiew, W.S. Chiu, Citric acid modified kenaf core fibers for removal of methylene blue from aqueous solution, Bioresour. Technol. 102 (2011) 7237–7243.
[50] A. Borazjani, S. Diehl, Kenaf core as an enhancer of bioremediation, in: C.E. Goforth, M.J. Fuller (Eds.), A Summary of Kenaf Production and Product Development Research. 1989–1993, Mississippi Agriculture and Forestry Experiment Station Bulletin 1011, Mississippi State University, 1994, pp. 26–27.
[51] H.M. Chol, M.C. Rinn, Natural sorbent in oil spill cleanups, Environ. Sci. Technol. 26 (1992) 772–776.
[52] M.O. Adebajo, R.L. Frost, J.T. Kloprogge, O. Carmody, Porous materials for oil spill cleanup: a review of synthesis and absorbing properties, J. Porous Mater. 10 (3) (2003) 159–170.
[53] T.D. Duong, M. Hoang, K.L. Nguyen, Sorption of Na+, Ca2+ ions from aqueous solution onto unbleached kraft fibers–kinetics and equilibrium studies, J. Col. Interface Sci. 287 (2005) 438–443.
[54] T.D. Duong, M. Hoang, K.L. Nguyen, Extension of donnan theory to predict calcium ion exchange on phenolic hydroxyl sites of unbleached kraft fibers, J. Colloid Interf. Sci. 276 (2004) 6–12.
[55] D.K. Mahmoud, M.A.M. Salleh, W.A.W. Abdul Karim, A. Idris, Z.Z. Abidin, Batch adsorption of basic dye using acid treated kenaf fibre char: equilibrium, kinetic and thermodynamic studies, J. Chem. Eng. 181–182 (2012) 449–457.

[56] X.C. Xu, C.S. Song, J.M. Andresen, B.G. Miller, A.W. Scaroni, Novel polyethylenimine–modified mesoporous molecular sieve of MCM–41 type as high capacity adsorbent for CO2 capture, Energy Fuel 16 (2002) 1463–1469.
[57] X. Wang, V. Schwartz, J.C. Clark, X. Ma, S.H. Overbury, X. Xu, C. Song, Infrared study of CO2 sorption over molecular basket sorbent consisting of polyethylenimine–modified mesoporous molecular sieve, J. Phys. Chem. C 113 (2009) 7260–7268.
[58] R. Serna–Guerrero, E. Da'na, A. Sayari, New insights into the interactions of CO_2 with amine–functionalized silica, Ind. Eng. Chem. Res. 47 (23) (2008) 9406–9412.
[59] V. Zelenak, D. Halamova, L. Gaberova, E. Bloch, P. Llewellyn, Amine –modified SBA–12 mesoporous silica for carbon dioxide capture: effect of amine basicity on sorption properties, Microporous Mesoporous Mater. 116 (1) (2008) 358–364.
[60] R. Chatti, A.K. Bansiwal, J.A. Thote, V. Kumar, P. Jadhav, S.K. Lokhande, R.B. Biniwale, N.K. Labhsetwar, S.S. Rayalu, Amine loaded zeolites for carbon dioxide capture: amine loading and adsorption studies, Microporous Mesoporous Mater. 121 (2009) 84–89.
[61] D.M. Ruthven, S. Farooq, K.S. Knaebel, Pressure Swing Adsorption, United States of America, VCH Publisher, 1994.
[62] L.J. Gibson, The hierarchical structure and mechanics of plant materials, J. R. Soc. Interface 9 (76) (2012) 2749–2766.
[63] S. Bishnoi, G.T. Rochelle, Absorption of carbon dioxide into aqueous piperazine: reaction kinetics: mass transfer and solubility, Chem. Eng. Sci. 55 (2000) 5531–5543.
[64] J. Xiao, C.W. Li, M.H. Li, Kinetics of absorption of carbon dioxide into aqueous solutions of 2–amino–2–methyl–1–propanol + monoethanolamine, Chem. Eng. Sci. 55 (2000) 161–175.
[65] C.H. Liao, M.H. Li, Kinetics of absorption of carbon dioxide into aqueous solutions of monoethanolamine + N–methyldiethanolamine, Chem. Eng. Sci. 57 (2002) 4569–4582.
[66] T. Filburn, J.J. Helble, R.A. Weiss, Development of supported ethanolamines and modified ethanolamines for CO_2 capture, Ind. Eng. Chem. Res. 44 (5) (2005) 1542–1546.
[67] M.O. Abdullah, I.A.W. Tan, L.S. Lim, Automobile adsorption air–conditioning system using oil palm biomass–based activated carbon: a review, Renew. Sust Energy Rev. 15 (4) (2011) 2061–2072.